International Journal of Pharmacology

Int. J. Pharmacol. **2025**; 21(6): 44200
https://doi.org/10.31083/IJP44200

Research Article

Topotecan-Mediated Effects on Immune Function and Survival Rate in a Nude Mouse Model of Non-Small Cell Lung Cancer via the PTEN/PI3K/GSK-3β Pathway

Chong Tian[1,2,3,4], Mei Li[1,2,3], Wang Li[1,2,3], Haipeng Yu[1,2,3,*]

[1]Department of Interventional Therapy, Tianjin Medical University Institute and Hospital, National Clinical Research Center for Cancer, 300000 Tianjin, China
[2]Tianjin's Clinical Research Center for Cancer, Tianjin Medical University Institute and Hospital, 300000 Tianjin, China
[3]Key Laboratory of Cancer Prevention and Therapy, Tianjin Medical University Institute and Hospital, 300000 Tianjin, China
[4]Department of Oncology, Tianjin Beichen Hospital, 300400 Tianjin, China
*Correspondence: haipengyutj@163.com (Haipeng Yu)
Academic Editor: Mehmet Ozaslan
Submitted: 27 September 2024 Revised: 18 November 2024 Accepted: 23 November 2024 Published: 30 October 2025

Abstract

Background and Objective: Topotecan (TPT) is a novel class of anti-tumor drugs known for its broad-spectrum anti-cancer activity and low toxicity. This study aimed to investigate the potential mechanisms through which TPT mediates the phosphatase and tensin homolog/phosphatidylinositol 3-kinase/glycogen synthase kinase-3β (PTEN/PI3K/GSH-3β) signaling pathway to affect survival and tumor growth in Non-Small Cell Lung Cancer (NSCLC) xenograft nude mice. **Materials and Methods**: A NSCLC nude mouse model was fabricated by subcutaneously injecting H1993 human NSCLC cells into the right axillary fossa. The mice were treated with cisplatin (DDP) and 0.5, 1.0 and 2.0 mg/kg of TPT. Tumor volume changes were monitored and assessments were performed on organ indices, immune function, tumor cell apoptosis, survival rates (SRs) and protein levels of components involved in the PTEN/PI3K/GSK-3β pathway in tumor tissues. One-way analysis of variance (ANOVA) or Chi-square tests were conducted using SPSS 23.0 to compare intergroup differences. **Results**: The SRs of nude mice treated with DDP and TPT markedly increased, with high-dose TPT treatment showing a drastically superior SR to DDP ($p < 0.05$). As the dose of TPT increased, the tumor volumes in the mice decreased markedly, and the indices of the thymus and spleen notably increased. Among T lymphocyte subsets, the proportion of $CD4^+$ cells and the $CD4^+/CD8^+$ ratio increased, while the proportion of $CD8^+$ cells decreased. Serum levels of interleukin-4, tumor necrosis factor (TNF)-α and interferon-γ increased. The apoptosis rate of tumor cells increased, and the relative expression level of PTEN in tumor tissue increased, whereas the levels of p-PI3K, p-PI3K/PI3K ratio, p-GSK-3β, and p-GSK-3β/GSK-3 ratio decreased ($p < 0.05$). **Conclusion**: TPT dose-dependently inhibited NSCLC growth by modulating T-cell subsets, enhancing immune function, and exerting antitumor effects through the PTEN/PI3K/GSK-3β pathway. The high-dose group (2.0 mg/kg) demonstrated superior efficacy compared to the cisplatin and low-dose groups, validating the importance of concentration gradient design in determining the optimal therapeutic window.

Keywords: Non-Small Cell Lung Cancer; Topotecan; T lymphocyte subsets; immune function; PTEN/PI3K/GSK-3β pathway

1. Introduction

Non-Small Cell Lung Cancer (NSCLC) constitutes over 85% of lung cancer (LC) cases [1]. Most NSCLC patients present with advanced disease at diagnosis, leading to a high incidence of distant metastasis post-curative surgery and poor prognosis. Advances in chemotherapy and the application of targeted therapies have markedly improved response rates and 5 years survival rates (SRs) for NSCLC. However, factors such as treatment resistance pose limitations to further research in various targeted therapies [2,3].

The Topotecan (TPT) is derived from camptothecin and inhibits DNA topoisomerase I. It binds with both the enzyme and DNA, blocking the repair of single-strand DNA breaks [4]. DNA topoisomerase I is a crucial enzyme involved in DNA replication and repair, responsible for unwinding DNA and inducing single-strand breaks while forming a single-strand DNA sheath between DNA strands. As a DNA topoisomerase I inhibitor, TPT binds to the enzyme and disrupts DNA replication and repair processes, preventing cancer cells from continuing to grow and divide [5]. In addition to direct inhibition of DNA topoisomerase I, TPT also induces DNA breaks, further exacerbating damage to cancer cells [6]. Moreover, TPT induces cell apoptosis (programmed cell death) and arrests cells from progressing from the G2 phase to the M phase (mitosis), thereby further suppressing tumor cell proliferation [7]. The TPT is primarily used clinically to treat diseases such as SCLC and metastatic ovarian cancer. As a chemotherapy agent, TPT demonstrates significant efficacy and can synergize with taxanes or platinum-based drugs to enhance anticancer activity. Takahashi *et al*. [8] confirmed in clinical treatment of SCLC patients that employing TPT alone or in combi-

nation with Berzosertib suggested negligible differences in progression-free survival and adverse reactions, but combination therapy notably extended overall survival. Edelman *et al*. [9], discovered that combining TPT with Irinotecan drastically extended SR in patients with recurrent/refractory SCLC. Baize *et al*. [10], also found that combining TPT with cisplatin chemotherapy increased SR in SCLC patients. Common severe adverse effects include neutropenia, thrombocytopenia and anemia. Currently, TPT is approved for NSCLC. Nevertheless, more research is needed to explore the efficacy and mechanisms of TPT in treating NSCLC.

This work established an NSCLC nude mouse model by subcutaneously injecting H1993 human NSCLC cells into the right axillary fossa. Effects of cisplatin (DDP) and different concentrations of TPT on SRs, immune function, tumor growth and tumor cell apoptosis in the nude mouse model were compared. The goal was to provide reference data for investigating the potential mechanisms of TPT in treating NSCLC.

2. Materials and Methods

2.1 Study Area

The research was performed at Tianjin Medical University Institute and Hospital (Tianjin, China) from January, 2023 to January, 2024.

2.2 Cell Culture

Human NSCLC cell line H1993 (obtained from ATCC, Manassas, VA, USA) was cultured in RPMI 1640 medium (Gibco, Grand Island, NY, USA) (+10% FBS and 1% penicillin-streptomycin (Gibco, Grand Island, NY, USA)). The cell line was validated by STR profiling and tested negative for mycoplasma. Cultures were maintained in a humidified atmosphere at 37 °C with 5% CO_2. Cells were used for experiments upon reaching the logarithmic growth phase, adjusted to 1×10^7 cells/mL in a single-cell suspension.

2.3 Animal Grouping and Intervention

A total of 100 clean-grade male BALB/c-Nu nude mice (Jiangsu Wukong Biotechnology Co. Ltd., Nanjing, China), weighing 18–20 g and aged 4–6 weeks, were selected for the study. The mice were kept in an animal facility at temperatures of 22–25 °C and a relative humidity of 55%. Mice had unrestricted access to food and water and were under a 12/12 hrs light/dark cycle, with 5 mice housed per cage.

The experimental protocol was approved by the Animal Ethical Committee of Tianjin Medical University Institute and Hospital (No. WDRY2022-K032). All the experimental protocols involved in the current investigation followed the Guide for the Care and Use of Laboratory Animals of the National Institutes of Health and the ARRIVE (Animal Research: Reporting of *in vivo* experiments) guidelines.

2.4 Study Design

The nude mice were randomly rolled into Ctrl group (CG), DDP group (DG), 0.5, 1.0 and 2.0 mg/kg TPT group (TG), with 20 mice per group. All mice were subcutaneously inoculated with 0.2 mL of H1993 cell suspension in the right axilla. When the tumor volume reached approximately 0.1 cm^3, the DG received intraperitoneal injections of 2 mg/kg DDP (Sigma-Aldrich, St. Louis, MO, USA) in 0.4 mL, twice per week for a total of 6 injections. The 0.5, 1.0 and 2.0 mg/kg TGs were orally gavaged with different concentrations of TPT daily for 30 consecutive days.

2.5 Evaluation of Tumor Volume and Organ Indices

After gastric gavage treatment, tumor volume was measured utilizing a caliper every five days and SRs of mice were recorded. At the treatment period end, surviving nude mice were anesthetized intraperitoneally with 40 mg/kg of 2% sodium pentobarbital (produced by Foshan Chemical Experiment Factory, Foshan, China) and euthanized by cervical dislocation under aseptic conditions. Tumors, spleens and thymi were harvested, washed with phosphate-buffered saline and prepared for further analysis. The spleen index and thymus index were calculated accordingly.

2.6 ELISA

Before euthanizing of mice, 4 mL of venous blood was collected and treated with sodium heparin as an anticoagulant. Serum was then processed for the detection of Interleukin (IL)-4, Tumor Necrosis Factor (TNF)-α and interferon (IFN)-γ levels utilizing an ELISA kit (Shanghai Beyotime Biological Technology Co. Ltd., Shanghai, China).

2.7 Detection of T Lymphocyte Subsets

Venous blood was collected and anticoagulated, followed by serum separation. Mouse anti-CD4 antibody (BioLegend, Cat# 100510, clone RM4-5) and mouse anti-CD8 antibody (BioLegend, Cat# 100708, clone 53-6.7) were separately added and incubated in the dark for 15 min. Subsequently, 250 µL of sterile water was added and $CD4^+$ and $CD8^+$ T lymphocyte subsets in peripheral blood were measured utilizing a CytoFLEX flow cytometer (Beckman Coulter, Brea, CA, USA). The $CD4^+/CD8^+$ ratio was calculated accordingly.

2.8 Measurement of Tumor Cell Apoptosis Rate

One-third of the tumor tissue was taken and minced with ophthalmic scissors and centrifugated at 1000 rpm for 5 min. Applying Annexin V FITC/PI apoptosis detection kit (Beijing AnnuoRun Biological Technology Co. Ltd., Beijing, China), cells were resuspended in pre-cooled binding buffer, then incubated in the dark at room temperature for 10 min with 5 µL each of Annexin V-FITC and PI work-

ing solution added. The apoptosis rate of tumor cells was measured utilizing a CytoFLEX flow cytometer (Beckman Coulter, Brea, CA, USA).

2.9 Western Blotting

The frozen tumor tissue was pulverized in liquid nitrogen. Total RNA was extracted employing radioimmunoprecipitation assay buffer (Cell Signaling Technology, Danvers, MA, USA) and RNA concentration was quantified with a bicinchoninic acid protein assay kit (Beyotime Biotechnology, Shanghai, China). Thirty micrograms of protein were loaded onto SDS-PAGE gels, separated and transferred to polyvinylidene fluoride membranes blocked with 5% non-fat milk, then probed overnight at 4 °C with primary antibodies (Abcam, Shanghai, China) against chromosome ten, Phosphatase and Tensin Homolog (PTEN) (ab32199), Phosphatidylinositol 3-kinase (PI3K) (ab40755), p-PI3K (ab182651), glycogen synthase kinase-3β (GSK-3β) (ab32391), p-GSK-3β (ab75814) and GAPDH (ab8245; 1:5000 dilution) (all from Abcam, Cambridge, UK) (1:1000 dilution). After membrane cleaning with Tris-buffered saline with Tween 20 (TBST), a mixture of horseradish peroxidase (HRP)-labeled goat anti-rabbit IgG secondary antibody (Cell Signaling Technology, Cat # 7074S, Danvers, MA, USA; 1:5000 dilution) and HRP-labeled goat anti-mouse IgG secondary antibody (Cell Signaling Technology, Cat # 7076S, Danvers, MA, USA; 1:5000 dilution) was incubated at 25 °C for 2 hours. Protein bands were visualized employing ECL (enhanced chemiluminescence) reagent (Beyotime Biotechnology, Shanghai, China) and band intensities were quantified with the WD-9413BX system (Beijing Liuyi Biotechnology Co. Ltd., Beijing, China), employing GAPDH as a loading control.

2.10 Statistical Methods

Data analysis utilized SPSS 23.0 (IBM Corp., Armonk, NY, USA). Continuous variables were expressed as mean $\pm$ standard deviation (Mean $\pm$ SD). Intergroup comparisons were performed using independent samples *t*-test, while multigroup comparisons were analyzed by one-way analysis of variance (one-way ANOVA). Appropriate post hoc multiple comparison methods (*e.g.*, Tukey's test or Dunnett's test) were selected based on homogeneity of variance. Categorical variables (n/%) were compared using the Chi-square test. Statistical significance was defined as $p < 0.05$.

3. Results

3.1 Impact of TPT on Tumor Volume in NSCLC Xenografts

A comparison of tumor volume changes in nude mice with NSCLC xenografts was conducted (Fig. 1a). As time progressed, tumor volumes increased in all groups. Tumor volumes greatly decreased in DG, 0.5, 1.0 and 2.0 mg/kg TG versus CG ($p < 0.05$). Particularly, tumor volumes in the 2.0 mg/kg TG were drastically smaller than in the other groups ($p < 0.05$). Subsequently, a comparison of tumor volume inhibition rates in nude mice with NSCLC xenografts (Fig. 1b) indicated a negligible difference in tumor volume inhibition rates between DG and 0.5 mg/kg TG ($p > 0.05$). The tumor volume inhibition rates in 1.0 and 2.0 mg/kg TG were notably superior to those in DG and 0.5 mg/kg TG, with 2.0 mg/kg TG exhibiting the highest inhibition rate ($p < 0.05$).

3.2 Influence of TPT on Organ Indices in Nude Mice With NSCLC Xenografts

Comparison of thymus index (Fig. 2a) and spleen index (Fig. 2b) among different groups of nude mice with NSCLC xenografts showed that DG suggested prominent decreases in both thymus and spleen indices versus CG. At the same time, 1.0 and 2.0 mg/kg TG exhibited drastic increases ($p < 0.05$). Thymus and spleen indices in 1.0 and 2.0 mg/kg TG were notably superior to those in DG and 0.5 mg/kg TG, with 2.0 mg/kg TG showing the highest indices ($p < 0.05$).

3.3 Effect of TPT on IL-4, TNF-α and IFN-γ Levels in Nude Mice With NSCLC Xenografts

Comparison of serum interleukin (IL)-4 (Fig. 3a), tumor necrosis factor (TNF)-α (Fig. 3b) and interferon (IFN)-γ (Fig. 3c) levels among different groups of nude mice with NSCLC xenografts showed that relative to CG, all other groups suggested drastic increases in serum IL-4, TNF-α and IFN-γ ($p < 0.05$). Negligible differences existed in these factors between DG and 1.0 mg/kg TG ($p > 0.05$). However, relative to DG and 0.5 and 1.0 mg/kg TG, 2.0 mg/kg TG exhibited drastic increases in these levels ($p < 0.05$).

3.4 Impact of TPT on T Lymphocyte Subset Levels in Nude Mice With NSCLC Xenografts

Serum $CD4^+$ ratio (Fig. 4a), $CD8^+$ ratio (Fig. 4b) and $CD4^+/CD8^+$ ratio (Fig. 4c) were compared among different groups of nude mice with NSCLC xenografts. Relative to CG, all other groups suggested drastic increases in $CD4^+$ ratio and $CD4^+/CD8^+$ ratio, while $CD8^+$ ratio was greatly decreased ($p < 0.05$). The T lymphocyte subset levels differed slightly between DG and 1.0 mg/kg TG ($p > 0.05$). Nevertheless, 2.0 mg/kg TG exhibited drastic increases in $CD4^+$ ratio and $CD4^+/CD8^+$ ratio versus DG and 0.5 and 1.0 mg/kg TG, along with a great decrease in $CD8^+$ ratio ($p < 0.05$).

3.5 Influence of TPT on Apoptosis of NSCLC Xenograft Cells

Comparison of tumor cell apoptosis rates among different groups of nude mice with NSCLC xenografts was shown in Fig. 5a,b. Tumor cell apoptosis rates were markedly increased in all groups except CG ($p < 0.05$). Tumor cell apoptosis rates differed slightly between DG and 1.0 mg/kg TG ($p > 0.05$). However, relative to DG and

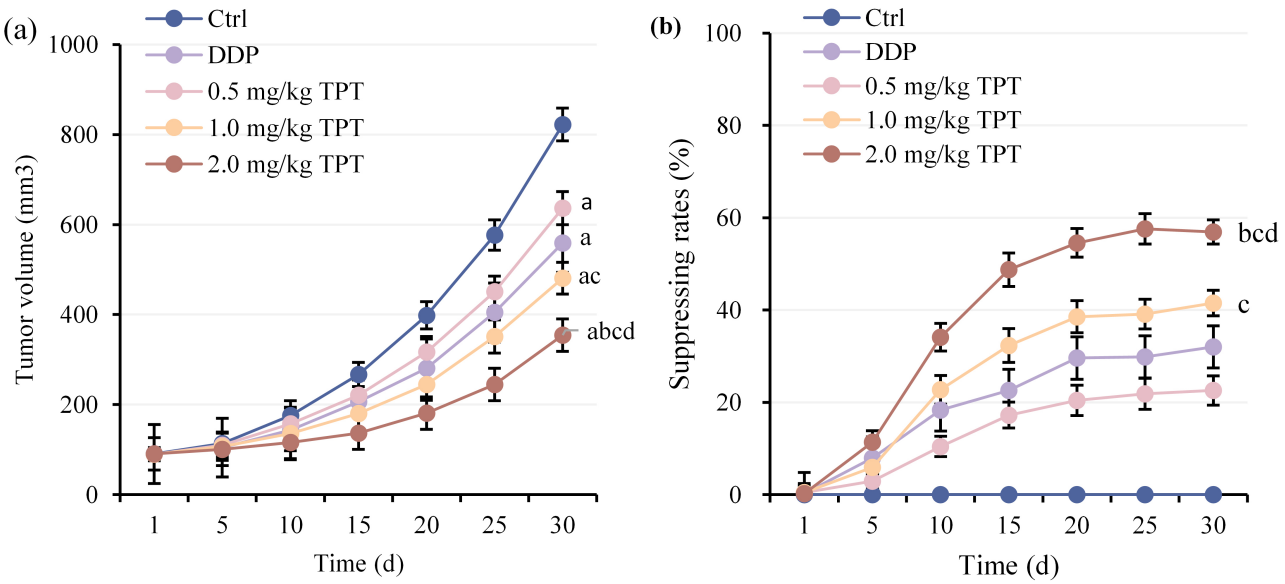

Fig. 1. Comparison of tumor volumes among groups of nude mice. (a) Tumor volume changes and (b) Tumor volume inhibition rate changes. $^{a}p < 0.05$ vs Ctrl group (CG), $^{b}p < 0.05$ vs DDP group (DG), $^{c}p < 0.05$ vs 0.5 mg/kg TPT group (TG) and $^{d}p < 0.05$ vs 1.0 mg/kg TG. DDP, cisplatin; TPT, Topotecan.

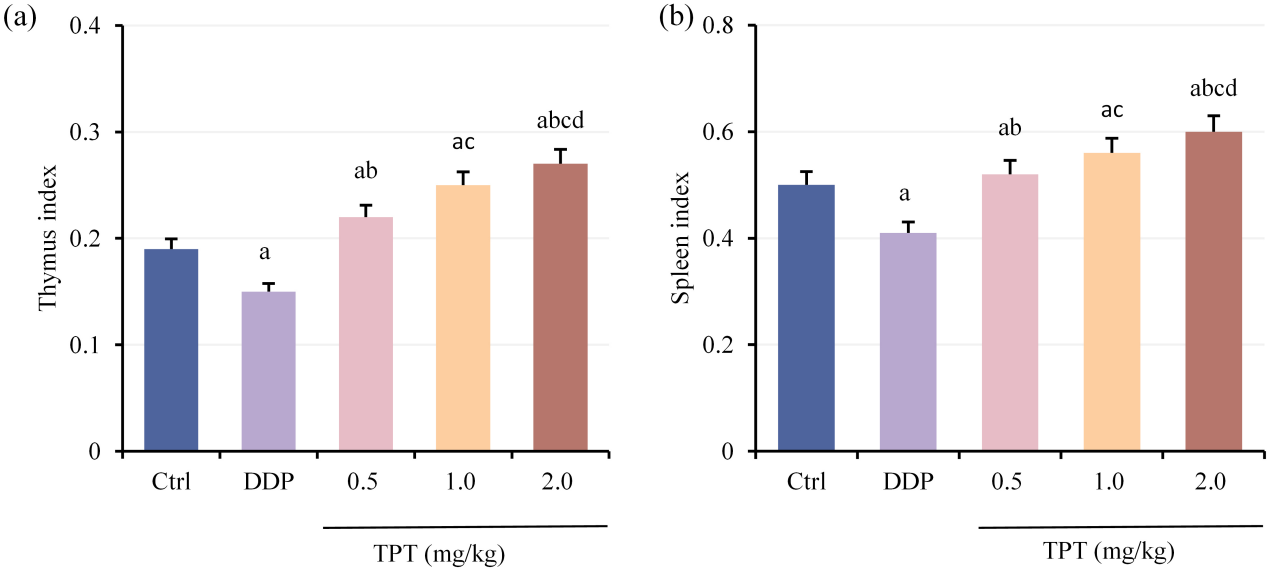

Fig. 2. Comparison of organ indices among groups of nude mice. (a) Thymus index and (b) Spleen index. $^{a}p < 0.05$ vs CG, $^{b}p < 0.05$ vs DG, $^{c}p < 0.05$ vs 0.5 mg/kg TG and $^{d}p < 0.05$ vs 1.0 mg/kg TG.

0.5 and 1.0 mg/kg TG, 2.0 mg/kg TG suggested a drastic increase in tumor cell apoptosis rate ($p < 0.05$).

3.6 Impact of TPT on SRs in Nude Mice With NSCLC Xenografts

Comparison of SRs among different groups of nude mice with NSCLC xenografts (Fig. 6) showed that SRs were markedly increased in all groups except CG ($p < 0.05$). There were negligible differences in SRs between DG and 1.0 mg/kg TG ($p > 0.05$). Nevertheless, 2.0 mg/kg TG suggested a drastic increase in SR versus DG and 0.5 and 1.0 mg/kg TG ($p < 0.05$).

3.7 Influence of TPT on PTEN/PI3K/GSK-3β Pathway in Nude Mice With NSCLC Xenografts

The relative expression levels of phosphatase and tensin homolog/phosphatidylinositol 3-kinase/glycogen synthase kinase-3β (PTEN/PI3K/GSK-3β) pathway-related proteins were compared among groups in NSCLC xenograft mice (Fig. 7a–f). Compared with CG, the expression levels of PTEN were significantly increased in

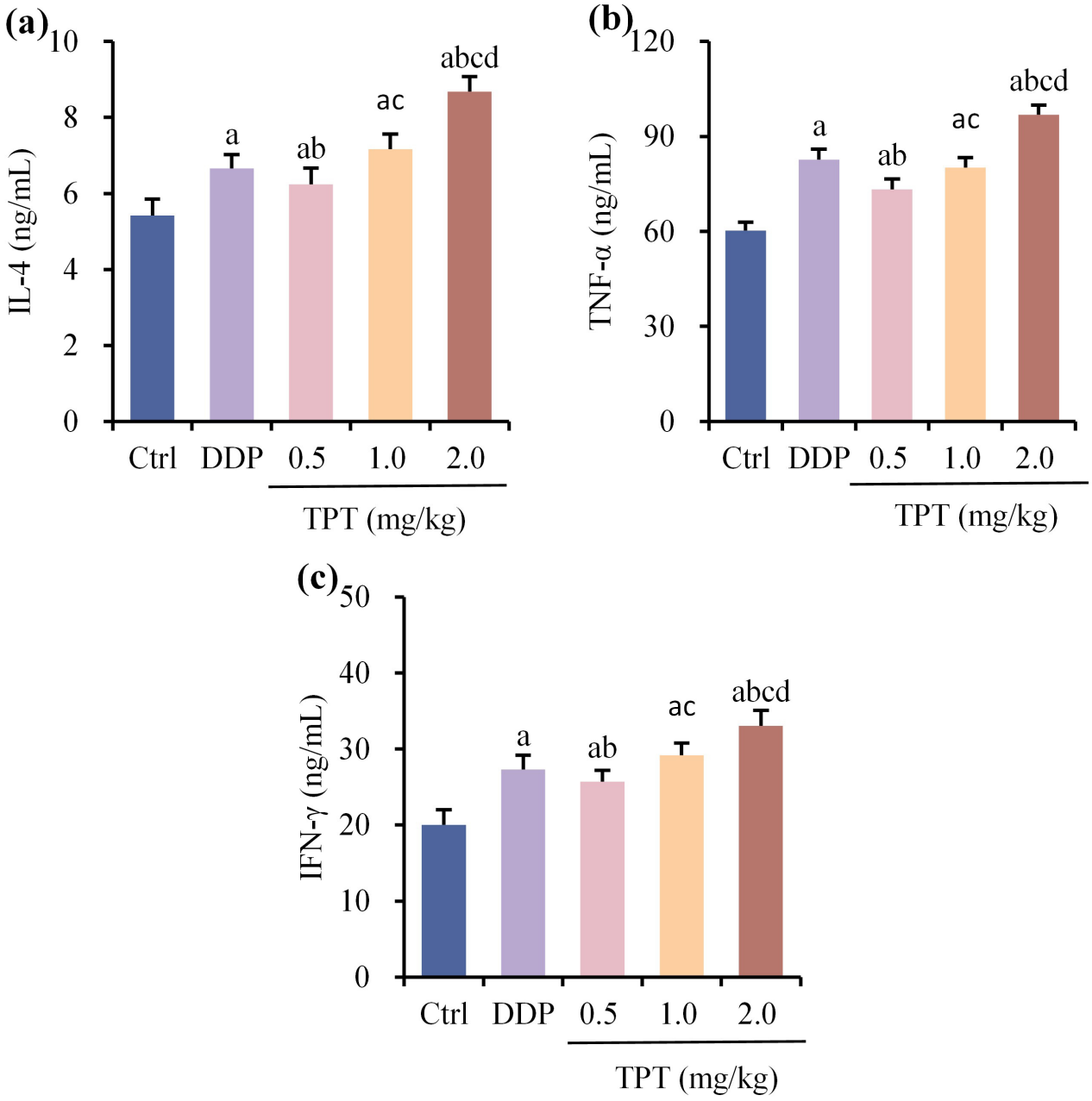

Fig. 3. Comparison of serum interleukin (IL)-4, tumor necrosis factor (TNF)-α and interferon (IFN)-γ among groups of nude mice. (a) IL-4 levels, (b) TNF-α levels and (c) IFN-γ levels. $^{a}p < 0.05$ vs CG, $^{b}p < 0.05$ vs DG, $^{c}p < 0.05$ vs 0.5 mg/kg TG and $^{d}p < 0.05$ vs 1.0 mg/kg TG.

all treatment groups, while the expression levels of p-PI3K, p-PI3K/PI3K ratio, p-GSK-3β, and p-GSK-3β/GSK-3β ratio were significantly decreased ($p < 0.05$). There was no significant difference ($p > 0.05$) in the expression of PTEN, p-PI3K, p-PI3K/PI3K ratio, p-GSK-3β, and p-GSK-3β/GSK-3β ratio between DG and the 1.0 mg/kg TG. However, PTEN expression was significantly higher in the 2.0 mg/kg TG than in the DG and 0.5 mg/kg and 1.0 mg/kg TGs, while the expression levels of p-PI3K, p-GSK-3β, p-PI3K/PI3K ratio, and p-GSK-3β/GSK-3β ratio were significantly reduced ($p < 0.05$). In addition, the p-PI3K/PI3K ratio and p-GSK-3β/GSK-3β ratio of the 2.0 mg/kg TG were the lowest among all groups ($p < 0.05$).

4. Discussion

The TPT was observed to drastically enhance SRs and suppress tumor volume growth in nude mice carrying NSCLC tumors, showing a dose-dependent response. The NSCLC arises from the bronchial mucosal epithelium. Most patients have grim prognosis and numerous complications [11]. The DDP is standard first-line therapy for advanced NSCLC, often combined with radiotherapy to ben-

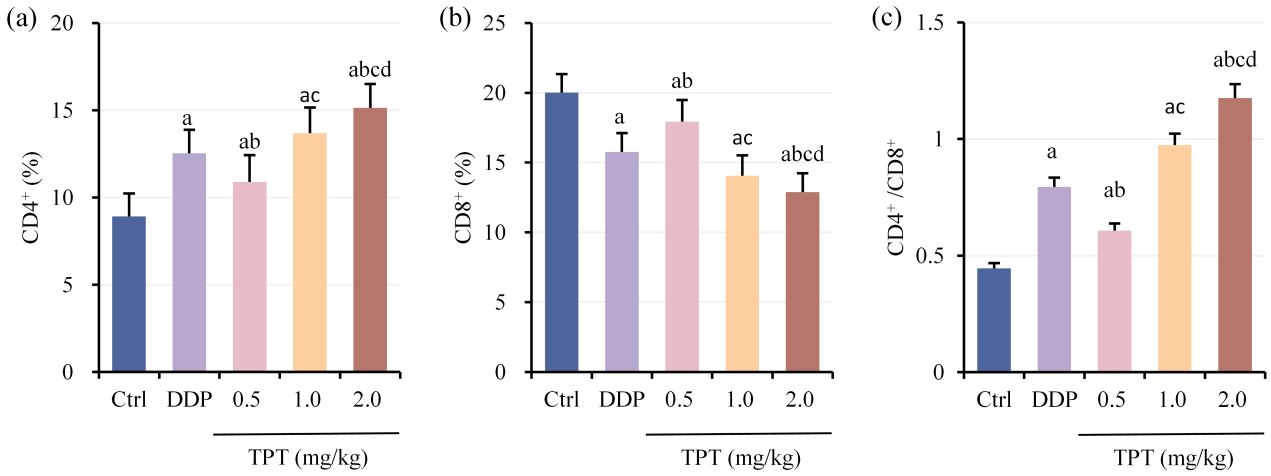

Fig. 4. Comparison of T lymphocyte subset levels among groups of nude mice. (a) $CD4^+$ cell proportion, (b) $CD8^+$ cell proportion and (c) $CD4^+/CD8^+$ ratio. [a]$p < 0.05$ vs CG, [b]$p < 0.05$ vs DG, [c]$p < 0.05$ vs 0.5 mg/kg TG and [d]$p < 0.05$ vs 1.0 mg/kg TG.

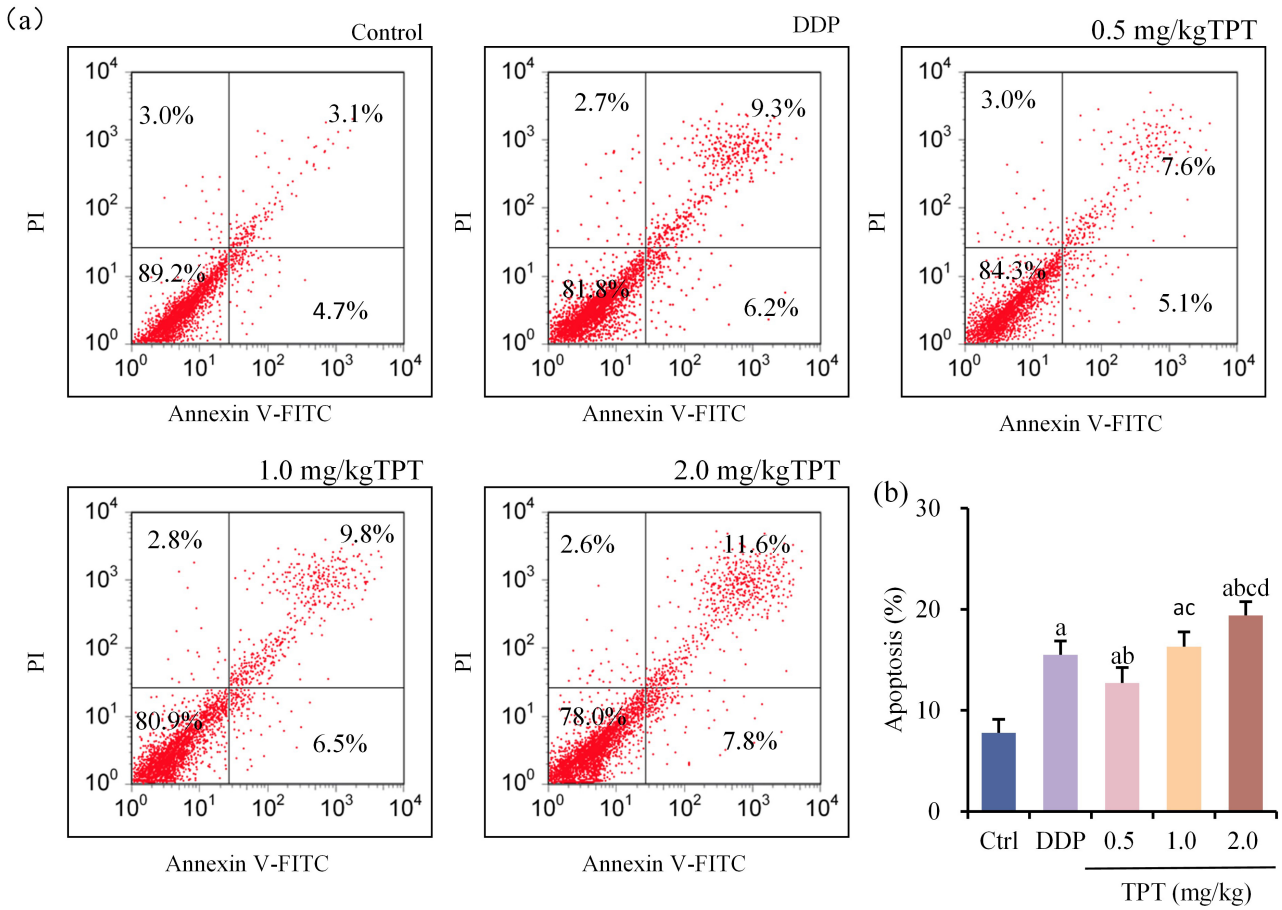

Fig. 5. Comparison of tumor cell apoptosis rates among groups of nude mice. (a) Flow cytometry plots for apoptosis detection and (b) Comparison of tumor cell apoptosis rates. [a]$p < 0.05$ vs CG, [b]$p < 0.05$ vs DG, [c]$p < 0.05$ vs 0.5 mg/kg TG and [d]$p < 0.05$ vs 1.0 mg/kg TG.

efit patients drastically [12,13]. Nevertheless, resistance to treatment can develop in some patients during therapy, which compromises its effectiveness. The mechanism of action of TPT in cancer treatment primarily involves inhibiting the activity of DNA topoisomerase I, thereby disrupting DNA replication and repair processes and inducing DNA breakage and cell apoptosis [14]. Zhang *et al.* [15], found that folate-conjugated TPT liposomes effectively re-

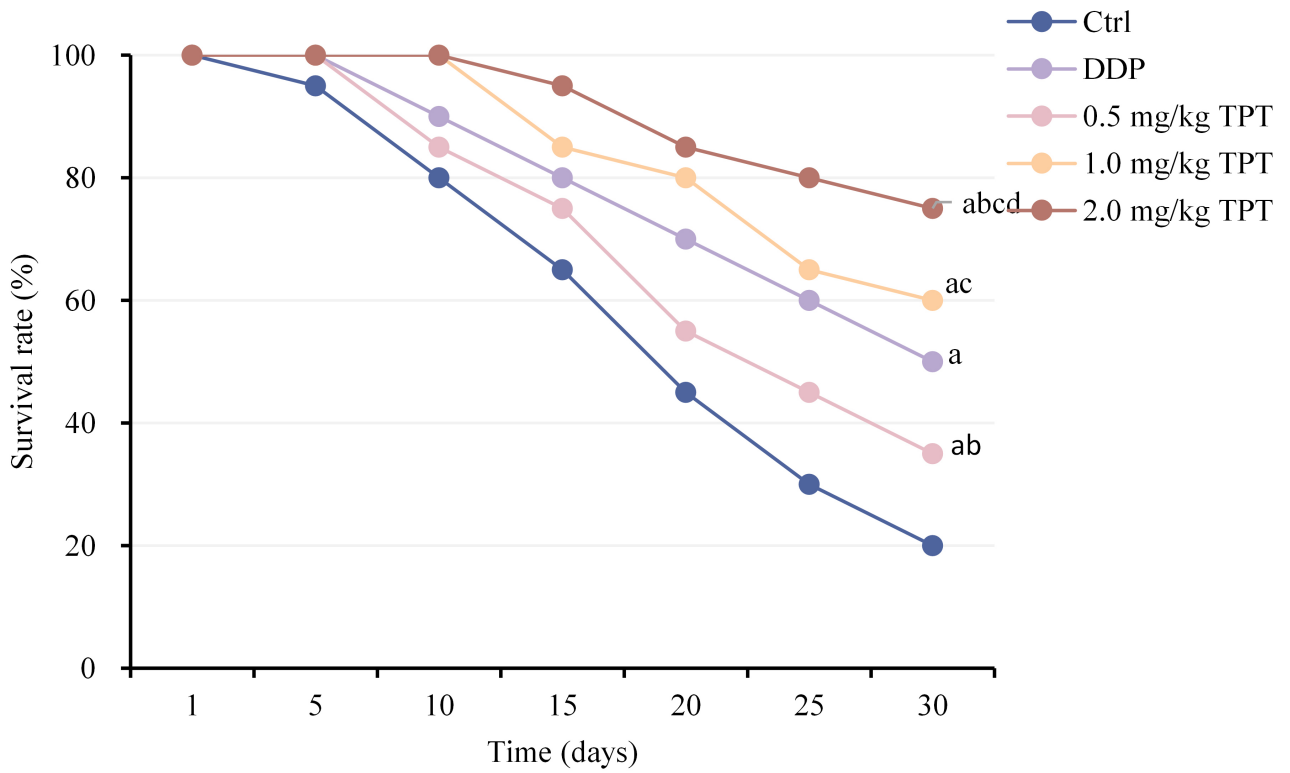

Fig. 6. Comparison of survival rates (SRs) among groups of nude mice. [a]$p < 0.05$ vs CG, [b]$p < 0.05$ vs DG, [c]$p < 0.05$ vs 0.5 mg/kg TG and [d]$p < 0.05$ vs 1.0 mg/kg TG.

duced tumor volume and prolonged circulation time in rats bearing A549 LC xenografts. However, the precise mechanism by which TPT treats NSCLC requires further exploration.

The thymus and spleen are crucial immune organs, integral to both central and peripheral immune systems [16]. It was observed that after treatment with DDP, the thymus and spleen indices decreased in nude mice bearing NSCLC tumors, indicating immune suppression in the host organism. Conversely, following administration of TPT, an increase in thymus and spleen indices was noted, showing a dose-dependent effect. This suggests that TPT can enhance thymus and spleen indices in nude mice bearing NSCLC tumors, thereby boosting both humoral and cellular immune functions. During the growth of LC cells, drastic immune evasion mechanisms exist, which are crucial factors in inducing LC development [17]. Changes in T lymphocyte subset levels can directly reflect the body's ability to inhibit tumor growth, including the major subsets $CD4^+$ and $CD8^+$ [18–20]. The $CD4^+$ T cells facilitate immune cell proliferation and differentiation and coordinate interactions among immune cells [21]. As key effector cells in anti-tumor immunity, $CD8^+$ cells typically inhibit tumor growth by directly killing tumor cells and secreting cytokines [22]. Conversely, an imbalance in the $CD4^+/CD8^+$ T-cell subset ratio or functional exhaustion of $CD8^+$ T cells may impair antitumor immunity, thereby facilitating tumor immune escape. It has been observed that after treatment with DDP and TPT, the peripheral blood $CD4^+$ cells and $CD4^+/CD8^+$ ratio markedly increased in nude mice bearing NSCLC tumors, while the proportion of $CD8^+$ cells decreased markedly. Particularly, treatment with high doses of TPT led to more pronounced changes in T lymphocyte subset levels. This suggests that TPT can correct abnormal T lymphocyte subset levels in the body, improve immune suppression and thereby drastically enhance immune function in nude mice bearing NSCLC tumors.

The IL-4 is an anti-inflammatory cytokine secreted by Th2 cells that promotes differentiation of Th0 cells into Th2 cells [23]. The TNF-α is a cytokine secreted by immune cells that markedly inhibits tumor cell growth and induces tumor regression [24]. The IFN-γ, produced by activated NK cells, is a Th1-type cytokine that suppresses the expression of pro-cancerous diseases and can hinder the transformation of tumor cells [25]. It has been observed that treatment with DDP and TPT increases IL-4, TNF-α and IFN-γ in the serum of nude mice bearing NSCLC, with TPT treatment exhibiting dose-dependent characteristics. The TNF-α can induce apoptosis and eliminate tumor cells, thereby inhibiting tumor growth [26]. The IFN-γ can activate various immune cells in the body, thereby directly killing tumor cells or indirectly inhibiting the expression of pro-cancerous diseases [27,28]. This indicates that TPT can inhibit T cell activation and proliferation and neg-

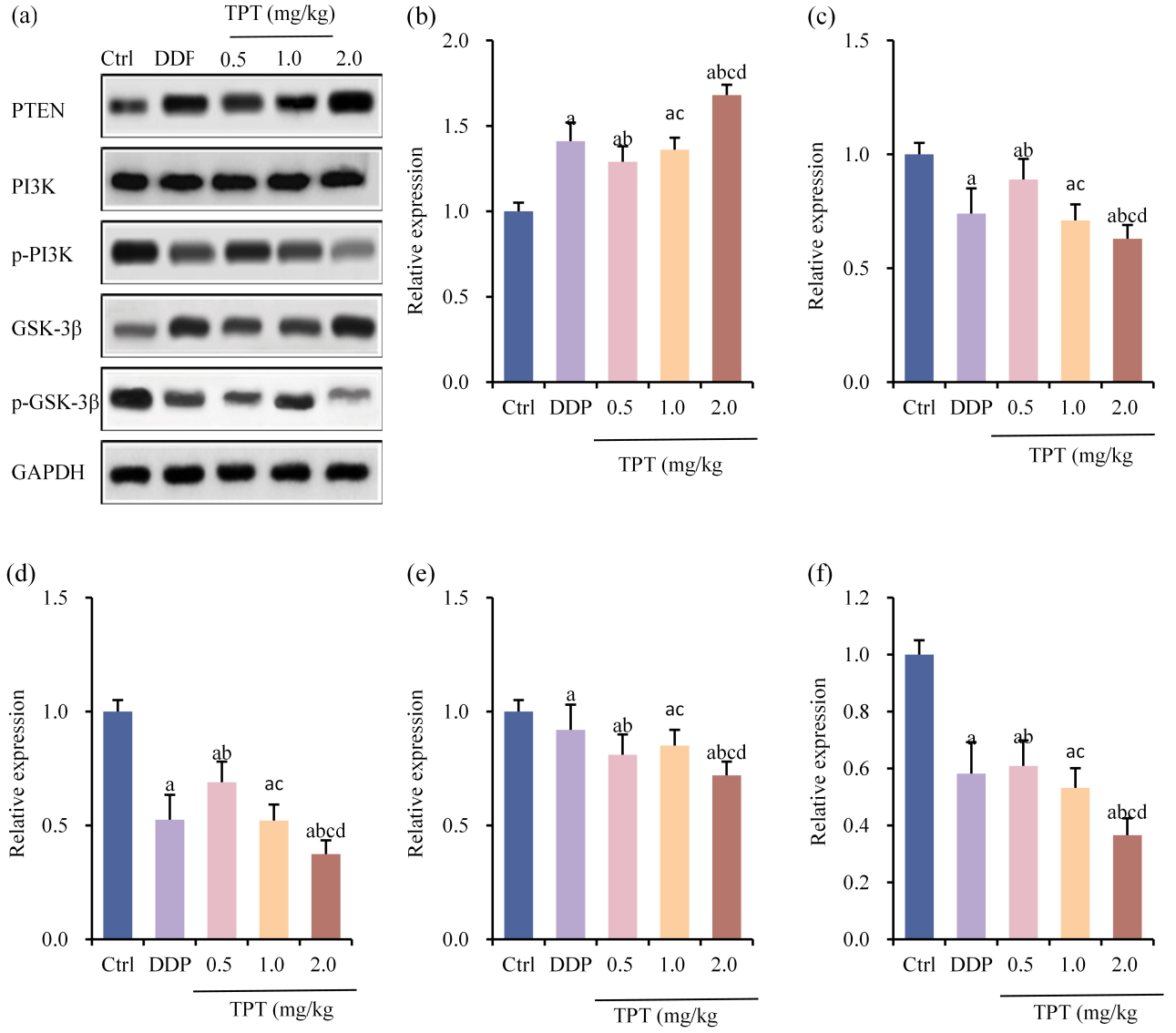

Fig. 7. Comparison of tumor PTEN/PI3K/GSK-3β pathway-related protein expressions among groups of nude mice. (a) Western blot detection images, (b) PTEN protein, (c) p-PI3K protein, (d) p-PI3K/PI3K protein, (e) p-GSK-3β protein and (f) p-GSK-3β/GSK-3β protein. $^{a}p < 0.05$ vs CG, $^{b}p < 0.05$ vs DG, $^{c}p < 0.05$ vs 0.5 mg/kg TG and $^{d}p < 0.05$ vs 1.0 mg/kg TG.

atively regulate immune escape of tumor cells after immune response by affecting IL-4, TNF-α and IFN-γ. Ultimately, it exerts cytotoxic effects on tumor cells through the body's immune mechanisms.

During tumor initiation and progression, dysregulated tumor suppressor gene phosphatase and tensin homolog deleted on PTEN can disrupt its normal control over the phosphatidylinositol 3-kinase/protein kinase B (PI3K/AKT) pathway. This disruption leads to unchecked cell proliferation, contributing to the development of cancer [29]. Abnormal PI3K/AKT pathway activation promotes the proliferation, migration and invasion of LC cells, facilitating disease progression [30]. Glycogen synthase kinase-3β (GSK-3β), as a downstream key effector molecule, not only participates in PI3K/AKT signaling, but also regulates tumor related pathways such as WNT/β-catenin [31,32]. When PTEN function is impaired or PI3K is continuously activated, GSK-3β is prone to phosphorylation inactivation (p-GSK-3β ↑), thereby weakening its induction of apoptosis and anticancer effects, promoting the survival and spread of tumor cells [33]. Conversely, upregulation of GSK-3β expression can inhibit the WNT/β-catenin pathway and promote apoptosis of LC cells [34]. This study indicates that both DDP and TPT can upregulate the expression of PTEN and GSK-3β in tumor tissues of NSCLC-bearing nude mice, significantly inhibit p-PI3K, p-PI3K/PI3K ratio, and p-GSK-3β and its ratio, suggesting that they can effectively inhibit the PI3K/AKT/GSK-3β pathway. Among them, TPT is dose-dependent, and the high-dose group has a better effect than DDP, showing

stronger anti-tumor activity. Morscher *et al*. [35], noted the same, who claimed that TPT in combination with Temozolomide can mediate the PI3K/AKT/mTOR pathway to treat pediatric cancers. These results indicate that TPT can inhibit the growth of NSCLC tumors by affecting the activity of the PTEN/PI3K/GSK-3β pathway.

The TPT, as a topoisomerase I inhibitor, holds significant importance in the study of NSCLC. This research demonstrates that TPT can correct the imbalance of T lymphocyte subsets by mediating the PTEN/PI3K/GSK-3β signaling pathway. This finding offers new perspectives and strategies for immunotherapy in lung cancer. The study not only enhances our understanding of the mechanisms underlying TPT's effects but also provides a theoretical foundation for developing more effective treatment regimens for lung cancer. Despite significant advances in the study of TPT in NSCLC, several limitations remain: (1) This study only compared the mechanisms of action of TPT monotherapy in Non-Small Cell Lung Cancer xenograft models; the potential enhanced efficacy of TPT in combination with other chemotherapeutic agents, such as DDP, requires further investigation. (2) Current research primarily focuses on xenograft models in mice and the applicability of these findings to human patients needs further validation and (3) The mechanisms of action of TPT warrant deeper investigation to understand its efficacy and safety in lung cancer treatment comprehensively. In summary, while the study of TPT in NSCLC is of significant importance and holds considerable promise for clinical application, it also faces limitations and challenges.

5. Conclusion

The TPT demonstrated dose-dependent characteristics in enhancing SRs and inhibiting tumor growth in nude mice with NSCLC xenografts. Its mechanism of action involves inducing tumor cell apoptosis, correcting imbalances in T lymphocyte subsets in nude mice, enhancing immune function and influencing the expression of PTEN, PI3K and GSK-3β proteins. Future research should continue to explore its mechanisms of action and optimize treatment protocols to improve outcomes and quality of life for lung cancer patients.

6. Significance Statement

This study investigated the efficacy of Topotecan in the treatment of Non-Small Cell Lung Cancer (NSCLC) via the PTEN/PI3K/GSK-3β Pathway, a critical area for advancing and developing novel approaches to enhance the therapeutic outcomes in NSCLC. Its unique and significant contribution lies in elucidating how topotecan modulates the immune system through specific intracellular signaling pathways, thereby effectively improving patient survival rates. This finding not only provides new insights into the complex interplay between cancer and the immune system but also paves the way for the development of innovative immunotherapeutic strategies in cancer treatment, potentially driving future advancements in the field.

Availability of Data and Materials

The datasets used and analyzed during the current study are available from the corresponding author on reasonable request.

Author Contributions

CT and HPY designed the research study. CT and HPY performed the research. CT, ML and WL analyzed the data. CT and HPY drafted and revised the manuscript. All authors contributed to editorial changes in the manuscript. All authors read and approved the final manuscript. All authors have participated sufficiently in the work and agreed to be accountable for all aspects of the work.

Ethics Approval and Consent to Participate

The experimental protocol was approved by the Animal Ethical Committee of Tianjin Medical University Institute and Hospital (No. WDRY2022-K032). All the experimental protocols involved in the current investigation followed the Guide for the Care and Use of Laboratory Animals of the National Institutes of Health and the ARRIVE (Animal Research: Reporting of *in vivo* experiments) guidelines.

Acknowledgment

Not applicable.

Funding

This research received no external funding.

Conflict of Interest

The authors declare no conflict of interest.

References

[1] Bertoli E, De Carlo E, Basile D, Zara D, Stanzione B, Schiappacassi M, *et al*. Liquid Biopsy in NSCLC: An Investigation with Multiple Clinical Implications. International Journal of Molecular Sciences. 2023; 24: 10803. https://doi.org/10.3390/ijms241310803.

[2] Alduais Y, Zhang H, Fan F, Chen J, Chen B. Non-small cell lung cancer (NSCLC): A review of risk factors, diagnosis, and treatment. Medicine. 2023; 102: e32899. https://doi.org/10.1097/MD.0000000000032899.

[3] Li Y, Juergens RA, Finley C, Swaminath A. Current and Future Treatment Options in the Management of Stage III NSCLC. Journal of Thoracic Oncology: Official Publication of the International Association for the Study of Lung Cancer. 2023; 18: 1478–1491. https://doi.org/10.1016/j.jtho.2023.08.011.

[4] Leavey PJ, Laack NN, Krailo MD, Buxton A, Randall RL, DuBois SG, *et al*. Phase III Trial Adding Vincristine-Topotecan-Cyclophosphamide to the Initial Treatment of Patients With Nonmetastatic Ewing Sarcoma: A Children's Oncology Group Report. Journal of Clinical Oncology: Official Journal of the

American Society of Clinical Oncology. 2021; 39: 4029–4038. https://doi.org/10.1200/JCO.21.00358.

[5] Alshammari MK, Alghazwni MK, Alharbi AS, Alqurashi GG, Kamal M, Alnufaie SR, *et al*. Nanoplatform for the Delivery of Topotecan in the Cancer Milieu: An Appraisal of its Therapeutic Efficacy. Cancers. 2022; 15: 65. https://doi.org/10.3390/cancers15010065.

[6] Koldysheva EV, Men'shchikova AP, Lushnikova EL, Popova NA, Kaledin VI, Nikolin VP, *et al*. Antimetastatic Activity of Combined Topotecan and Tyrosyl-DNA Phosphodiesterase-1 Inhibitor on Modeled Lewis Lung Carcinoma. Bulletin of Experimental Biology and Medicine. 2019; 166: 661–666. https://doi.org/10.1007/s10517-019-04413-3.

[7] Gasimli K, Raab M, Becker S, Sanhaji M, Strebhardt K. The Role of DAPK1 in the Cell Cycle Regulation of Cervical Cancer Cells and in Response to Topotecan. Journal of Cancer. 2022; 13: 728–743. https://doi.org/10.7150/jca.66492.

[8] Takahashi N, Hao Z, Villaruz LC, Zhang J, Ruiz J, Petty WJ, *et al*. Berzosertib Plus Topotecan vs Topotecan Alone in Patients With Relapsed Small Cell Lung Cancer: A Randomized Clinical Trial. JAMA Oncology. 2023; 9: 1669–1677. https://doi.org/10.1001/jamaoncol.2023.4025.

[9] Edelman MJ, Dvorkin M, Laktionov K, Navarro A, Juan-Vidal O, Kozlov V, *et al*. Randomized phase 3 study of the anti-disialoganglioside antibody dinutuximab and irinotecan vs irinotecan or topotecan for second-line treatment of small cell lung cancer. Lung Cancer (Amsterdam, Netherlands). 2022; 166: 135–142. https://doi.org/10.1016/j.lungcan.2022.03.003.

[10] Baize N, Monnet I, Greillier L, Geier M, Lena H, Janicot H, *et al*. Carboplatin plus etoposide versus topotecan as second-line treatment for patients with sensitive relapsed small-cell lung cancer: an open-label, multicentre, randomised, phase 3 trial. The Lancet. Oncology. 2020; 21: 1224–1233. https://doi.org/10.1016/S1470-2045(20)30461-7.

[11] Ettinger DS, Wood DE, Aisner DL, Akerley W, Bauman JR, Bharat A, *et al*. Non-Small Cell Lung Cancer, Version 3.2022, NCCN Clinical Practice Guidelines in Oncology. Journal of the National Comprehensive Cancer Network: JNCCN. 2022; 20: 497–530. https://doi.org/10.6004/jnccn.2022.0025.

[12] Kryczka J, Kryczka J, Czarnecka-Chrebelska KH, Brzeziańska-Lasota E. Molecular Mechanisms of Chemoresistance Induced by Cisplatin in NSCLC Cancer Therapy. International Journal of Molecular Sciences. 2021; 22: 8885. https://doi.org/10.3390/ijms22168885.

[13] Zhong WZ, Wang Q, Mao WM, Xu ST, Wu L, Wei YC, *et al*. Gefitinib Versus Vinorelbine Plus Cisplatin as Adjuvant Treatment for Stage II-IIIA (N1-N2) EGFR-Mutant NSCLC: Final Overall Survival Analysis of CTONG1104 Phase III Trial. Journal of Clinical Oncology: Official Journal of the American Society of Clinical Oncology. 2021; 39: 713–722. https://doi.org/10.1200/JCO.20.01820.

[14] Upadhyayula PS, Spinazzi EF, Argenziano MG, Canoll P, Bruce JN. Convection Enhanced Delivery of Topotecan for Gliomas: A Single-Center Experience. Pharmaceutics. 2020; 13: 39. https://doi.org/10.3390/pharmaceutics13010039.

[15] Zhang J, Shi W, Xue G, Ma Q, Cui H, Zhang L. Improved Therapeutic Efficacy of Topotecan Against A549 Lung Cancer Cells with Folate-targeted Topotecan Liposomes. Current Drug Metabolism. 2020; 21: 902–909. https://doi.org/10.2174/1389200221999200820163337.

[16] Han Y, Shi S, Liu S, Gu X. Effects of spaceflight on the spleen and thymus of mice: Gene pathway analysis and immune infiltration analysis. Mathematical Biosciences and Engineering: MBE. 2023; 20: 8531–8545. https://doi.org/10.3934/mbe.2023374.

[17] Anichini A, Perotti VE, Sgambelluri F, Mortarini R. Immune Escape Mechanisms in Non Small Cell Lung Cancer. Cancers. 2020; 12: 3605. https://doi.org/10.3390/cancers12123605.

[18] He L, Wang J, Chang D, Lv D, Li H, Zhang H. Clinical value of Pro-GRP and T lymphocyte subpopulation for the assessment of immune functions of lung cancer patients after DC-CIK biological therapy. Experimental and Therapeutic Medicine. 2018; 15: 1580–1585. https://doi.org/10.3892/etm.2017.5520.

[19] Gueguen P, Metoikidou C, Dupic T, Lawand M, Goudot C, Baulande S, *et al*. Contribution of resident and circulating precursors to tumor-infiltrating $CD8^+$ T cell populations in lung cancer. Science Immunology. 2021; 6: eabd5778. https://doi.org/10.1126/sciimmunol.abd5778.

[20] Salazar Y, Zheng X, Brunn D, Raifer H, Picard F, Zhang Y, *et al*. Microenvironmental Th9 and Th17 lymphocytes induce metastatic spreading in lung cancer. The Journal of Clinical Investigation. 2020; 130: 3560–3575. https://doi.org/10.1172/JCI124037.

[21] Xie M, Wei J, Xu J. Inducers, Attractors and Modulators of $CD4^+$ Treg Cells in Non-Small-Cell Lung Cancer. Frontiers in Immunology. 2020; 11: 676. https://doi.org/10.3389/fimmu.2020.00676.

[22] Chow A, Uddin FZ, Liu M, Dobrin A, Nabet BY, Mangarin L, *et al*. The ectonucleotidase CD39 identifies tumor-reactive $CD8^+$ T cells predictive of immune checkpoint blockade efficacy in human lung cancer. Immunity. 2023; 56: 93–106.e6. https://doi.org/10.1016/j.immuni.2022.12.001.

[23] Yan X, Li W, Pan L, Fu E, Xie Y, Chen M, *et al*. Lewis Lung Cancer Cells Promote SIGNR1(CD209b)-Mediated Macrophages Polarization Induced by IL-4 to Facilitate Immune Evasion. Journal of Cellular Biochemistry. 2016; 117: 1158–1166. https://doi.org/10.1002/jcb.25399.

[24] Chan SH, Kuo WH, Wang LH. SCEL regulates switches between pro-survival and apoptosis of the TNF-α/TNFR1/NF-κB/c-FLIP axis to control lung colonization of triple negative breast cancer. Journal of Biomedical Science. 2023; 30: 93. https://doi.org/10.1186/s12929-023-00986-4.

[25] Fang C, Weng T, Hu S, Yuan Z, Xiong H, Huang B, *et al*. IFN-γ-induced ER stress impairs autophagy and triggers apoptosis in lung cancer cells. Oncoimmunology. 2021; 10: 1962591. https://doi.org/10.1080/2162402X.2021.1962591.

[26] Terlizzi M, Colarusso C, Somma P, De Rosa I, Panico L, Pinto A, *et al*. S1P-Induced TNF-α and IL-6 Release from PBMCs Exacerbates Lung Cancer-Associated Inflammation. Cells. 2022; 11: 2524. https://doi.org/10.3390/cells11162524.

[27] Pan H, Chai W, Liu X, Yu T, Sun L, Yan M. DYNC1H1 regulates NSCLC cell growth and metastasis by IFN-γ-JAK-STAT signaling and is associated with an aberrant immune response. Experimental Cell Research. 2021; 409: 112897. https://doi.org/10.1016/j.yexcr.2021.112897.

[28] Hu WT, Zhang Q, Zhang Z, He X, Zhou M, Guo Y, *et al*. Eosinophil and IFN-γ associated with immune-related adverse events as prognostic markers in patients with non-small cell lung cancer treated with immunotherapy. Frontiers in Immunology. 2023; 14: 1112409. https://doi.org/10.3389/fimmu.2023.1112409.

[29] Braglia L, Zavatti M, Vinceti M, Martelli AM, Marmiroli S. Deregulated PTEN/PI3K/AKT/mTOR signaling in prostate cancer: Still a potential druggable target? Biochimica et Biophysica Acta. Molecular Cell Research. 2020; 1867: 118731. https://doi.org/10.1016/j.bbamcr.2020.118731.

[30] Gulhane P, Singh S. MicroRNA-520c-3p impacts sphingolipid metabolism mediating PI3K/AKT signaling in NSCLC: Systems perspective. Journal of Cellular Biochemistry. 2022; 123: 1827–1840. https://doi.org/10.1002/jcb.30319.

[31] Yang W, Liu Y, Xu QQ, Xian YF, Lin ZX. Sulforaphene Ameliorates Neuroinflammation and Hyperphosphorylated Tau Pro-

tein via Regulating the PI3K/Akt/GSK-3β Pathway in Experimental Models of Alzheimer's Disease. Oxidative Medicine and Cellular Longevity. 2020; 2020: 4754195. https://doi.org/10.1155/2020/4754195.

[32] Lin J, Song T, Li C, Mao W. GSK-3β in DNA repair, apoptosis, and resistance of chemotherapy, radiotherapy of cancer. Biochimica et Biophysica Acta. Molecular Cell Research. 2020; 1867: 118659. https://doi.org/10.1016/j.bbamcr.2020.118659.

[33] Sirhan Z, Alojair R, Thyagarajan A, Sahu RP. Therapeutic Implications of PTEN in Non-Small Cell Lung Cancer. Pharmaceutics. 2023; 15: 2090. https://doi.org/10.3390/pharmaceutics15082090.

[34] Liu Q, Luo Z, Yang J. Polyphyllin III regulates EMT of lung cancer cells through GSK-3β/β-catenin pathway. Annals of Medicine and Surgery (2012). 2024; 86: 1376–1385. https://doi.org/10.1097/MS9.0000000000001629.

[35] Morscher RJ, Brard C, Berlanga P, Marshall LV, André N, Rubino J, *et al*. First-in-child phase I/II study of the dual mTORC1/2 inhibitor vistusertib (AZD2014) as monotherapy and in combination with topotecan-temozolomide in children with advanced malignancies: arms E and F of the AcSé-ESMART trial. European Journal of Cancer (Oxford, England: 1990). 2021; 157: 268–277. https://doi.org/10.1016/j.ejca.2021.08.010.